

Review

# Numerical Modelling of Forced Convection of Nanofluids in Smooth, Round Tubes: A Review

Janusz T. Cieśliński 

Faculty of Mechanical and Ocean Engineering, Gdańsk University of Technology, Narutowicza 11/12, 80233 Gdansk, Poland; jcieslin@pg.edu.pl

**Abstract:** A comprehensive review of published works dealing with numerical modelling of forced convection heat transfer and hydrodynamics of nanofluids is presented. Due to the extensive literature, the review is limited to straight, smooth, circular tubes, as this is the basic geometry in shell-and-tube exchangers. Works on numerical modelling of forced convection in tubes are presented chronologically in the first part of the article. Particular attention was paid to the method of the solution of governing equations, geometry of the heating section, and boundary conditions assumed. Influence of nanoparticles on heat transfer and flow resistance are discussed. Basic information is summarized in tabular form, separately for single-phase approach and two-phase models. The second part of the article contains the correlation equations proposed in the presented papers for the calculation of the Nusselt (Nu) number or heat transfer coefficient, separately for laminar and turbulent flow. Details of the type of nanofluids, the concentration of nanoparticles, and the Reynolds (Re) number range are also presented. Finally, advantages and disadvantages of individual numerical approaches are discussed.

**Keywords:** forced convection; nanofluids; straight; smooth; round tubes; heat transfer; flow resistance



**Citation:** Cieśliński, J.T. Numerical Modelling of Forced Convection of Nanofluids in Smooth, Round Tubes: A Review. *Energies* **2022**, *15*, 7586. <https://doi.org/10.3390/en15207586>

Academic Editor: Gianpiero Colangelo

Received: 13 September 2022

Accepted: 10 October 2022

Published: 14 October 2022

**Publisher's Note:** MDPI stays neutral with regard to jurisdictional claims in published maps and institutional affiliations.



**Copyright:** © 2022 by the author. Licensee MDPI, Basel, Switzerland. This article is an open access article distributed under the terms and conditions of the Creative Commons Attribution (CC BY) license (<https://creativecommons.org/licenses/by/4.0/>).

## 1. Introduction

Nanofluids are one of the techniques for heat transfer enhancement [1,2]. The goal is obvious: to reduce the heat transfer surface area, thus reducing the consumption of materials and energy necessary for the manufacture of heat exchangers. However, in order for nanofluids to find practical applications, several problems must be solved. The first and foremost is to provide engineers with accurate and reliable methods to calculate heat transfer coefficients and friction factors. The second problem is the thermophysical properties of nanofluids, the determination of which is not easy [3,4]. The third problem that has so far held back the practical application of nanofluids is their stability [5,6]. Due to the costs of experimental research and the long design and construction time of measuring stands, as well as tedious measurements, numerical methods are an indispensable approach that allow for quick and precise assessment of new technologies. However, it should be remembered that each numerical work should be verified experimentally or, if possible, by an analytical solution. There are two main approaches in the modeling of nanofluid flows, e.g., [7–11]. Due to the size of nanoparticles (similar to the dimensions of liquid molecules), it is assumed that the resulting mixture forms a homogeneous liquid, the properties of which result from the properties of the base liquid and solid particles. Hence, the classical methods of continuum mechanics are used to solve the set of governing equations. In the second approach, a nanofluid is treated as two phase solid-liquid mixture.

This paper presents state of the art in the field of numerical modeling of the forced convection of nanofluids in straight, smooth, round tubes.

## 2. Methods

Maïga et al. [12] considered the problem of nanofluid flow inside a uniformly heated tube and applied a single-phase approach. In general, it was observed that the inclusion

of nanoparticles considerably enhanced heat transfer for both the laminar and turbulent regimes. Such improvement of heat transfer becomes more pronounced with the increase of the nanoparticle concentration (NPC). On the other hand, the presence of particles has produced adverse effects on the wall friction that also increases with the NPC. In [13], Maïga et al. studied the laminar flow of nanofluids inside a uniformly heated tube. It was shown that the presence of nanoparticles induced drastic effects on the wall shear stress (WSS) that increased appreciably with the NPC increase. In [14], Maïga et al. studied the turbulent flow of nanofluids inside a uniformly heated tube. A single-phase approach was used to solve the system of non-linear and coupled governing equations, and the  $k-\varepsilon$  model was employed in order to model the turbulence. It was found that HTC increases with NPC increase. Heris et al. [15] investigated the laminar flow of nanofluid in an isothermal tube. A dispersion model with constant thermophysical properties of nanofluids were assumed. Heat transfer enhancement was detected with NPC increase. Moreover, the Nu number decreased with nanoparticle diameter increase for the given NPC. Behzadmehr et al. [16] studied the turbulent flow of nanofluids in a uniformly heated tube. Probably for the first time, a mixture model was applied to study nanofluid behavior. It was found that the mixture model better interpreted experimental results than the single-phase approach. Bianco et al. [17] studied laminar flow of nanofluids for a single value of the Re number in a uniformly heated tube. A single-phase approach and the discrete particles model were employed with either constant or temperature-dependent properties. Heat transfer enhancement was observed with NPC increase. In [18], Bianco et al. investigated developing the laminar flow of nanofluid in a circular, uniformly heated tube. A single-phase approach and two-phase model (discrete particles model) were employed with either constant or temperature-dependent properties. The maximum difference in the average HTC between single-phase and two-phase models was about 11%. Heat transfer enhancement increases with the NPC increase, but it is accompanied by increasing WSS. Higher HTC and lower WSS were detected in the case of temperature dependent models. In Figure 1 results of numerical calculations by use of single-phase (1Phase) approach and DPM model with constant (con.) and variable (var.) thermophysical properties of nanofluid are shown.

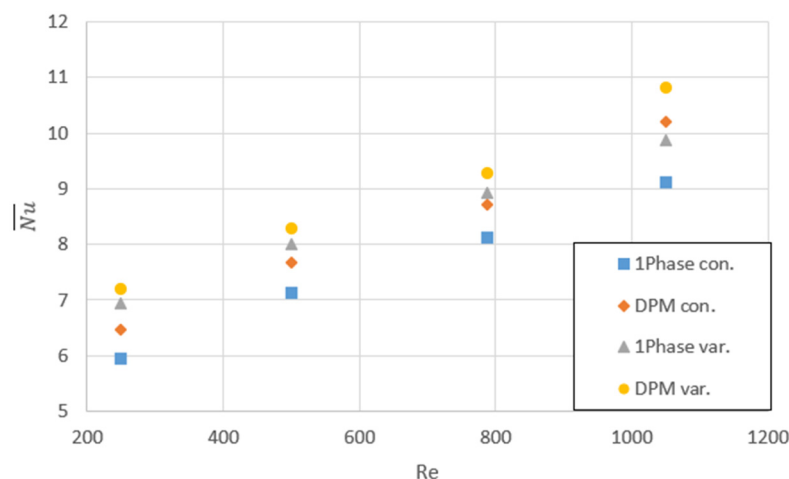


**Figure 1.**  $\overline{Nu}$ -Re relationship for water- $\gamma\text{Al}_2\text{O}_3$  (1%) nanofluid—data source [18].

He et al. [19] studied the heat transfer of nanofluids flowing through a straight tube under laminar flow conditions by using both the single-phase method and combined Euler-Lagrange method. The results show significant enhancement of heat transfer of nanofluids particularly in the entrance region. The results suggest that the HTC is more affected by the thermal conductivity than by the viscosity and the Brownian force; the lift force and the thermophoretic force play very small role. Namburu et al. [20] analyzed the turbulent flow of nanofluids flowing through a circular tube under a constant heat flux condition. The nanofluids were considered as a conventional single-phase fluid. The thermophysical



properties are dependent upon the temperature and NPC. It was found that nanofluids containing smaller diameter nanoparticles have higher viscosity and Nu numbers. Fard et al. [21] studied the laminar convective heat transfer of nanofluids in a circular tube under a constant wall temperature condition. Single-phase and two-phase models were used for the prediction of temperature, flow field, and calculation of HTC. The results showed that HTC increases with an increase in NPC, and the heat transfer enhancement increases with Pelet (Pe) number. The two-phase model shows better agreement with experimental measurements. Based on the results of the CFD simulation, it was concluded that the two-phase approach gives better predictions for heat transfer rate compared to the single-phase model. Lotfi et al. [22] studied the forced convection of a nanofluid in a horizontal uniformly heated tube. A two-phase Eulerian model was implemented to study a flow field. A single-phase model and two-phase mixture model were also used. The comparison of calculated results with experimental values shows that the mixture model is more precise. It is illustrated that the single-phase model and the two-phase Eulerian model underestimates the Nu number in comparison with the experimental data. Figure 2 shows a comparison of numerical calculations by use of single-phase (1Phase) approach and two two-phase models, namely a mixture model (Mixture) and Eulerian (E) model.

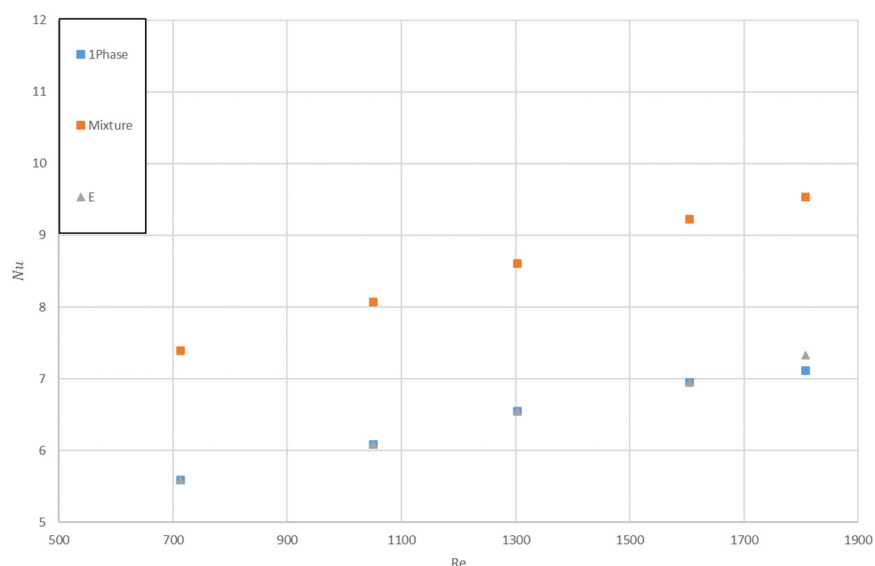


**Figure 2.** Nu-Re relationship for water–Al<sub>2</sub>O<sub>3</sub> (1%) nanofluid and  $x/D = 63$ —data source [22].

Mokmeli and Saffar-Avval [23] studied the laminar flow of nanofluids in uniformly heated and isothermal tubes. A single-phase approach and dispersion model were used to simulate the effect of nanoparticle diameter and NPC on heat transfer. It was established that HTC increases with the decrease of nanoparticles, and the single-phase model, contrary to the dispersion model, predicts the decrease of the Nu number against NPC. It was shown that dispersion model better reproduces experimental data. Ebrahimnia-Bajestan et al. [24] analyzed the effects of NPC, particle diameter, Brownian motion, Re number, type of nanoparticles and base fluid on the HTC and pressure drop (PD) of nanofluids during laminar flow at constant heat flux boundary condition. A single-phase model was used to simulate nanofluid behavior. It was established that HTC increases with NPC and aspect ratio increase, and decreases with nanoparticle diameter increase. Moraveji et al. [25] studied the influence of nanoparticle diameter on HTC in the developing region of a tube using the single-phase nanofluid model. Laminar flow with a constant heat flux boundary condition was examined. It was established that HTC deteriorated with an increase in the axial location and particle diameter. Bianco et al. [26] studied the turbulent flow of nanofluids in uniformly heated tube using the single-phase approach and mixture model. Constant thermophysical properties of nanofluids with standard  $k-\epsilon$  turbulence model were applied. The authors emphasized the importance of correctly determining the properties of

nanofluids. Bayat and Nikseresht [27] studied the effect of type of nanofluid on PD and heat transfer during laminar flow in a uniformly heated tube. The single-phase approach with temperature and NPC dependent properties of nanofluids was applied. The most important conclusion is that it is possible to enhance heat transfer with lower WSS by the selection of a proper nanofluid. Akbari et al. [28] applied a single-phase and three different two-phase models (VOF, mixture, Eulerian) to analyze the laminar convection of nanofluids in a horizontal tube with uniform wall heat flux. The predictions by the three two-phase models were essentially the same. The two-phase models give closer predictions of the HTC to the experimental data than the single-phase model. In [29] Akbari et al. used the same numerical approaches as in [28] but this time studied the turbulent flow of nanofluids in a horizontal tube with uniform wall heat flux. It was established that the predictions by the single-phase model and by the two-phase models favors the single-phase approach. Since the single-phase model is also simpler to implement and requires less computer memory and CPU time, it was concluded that it is more appropriate for the conditions under study. Figure 3 shows comparison of numerical calculations by use of single-phase (1Phase) approach and three two-phase models, namely Eulerian (E) model, mixture model (Mixture), and volume of fluid model (VOF).

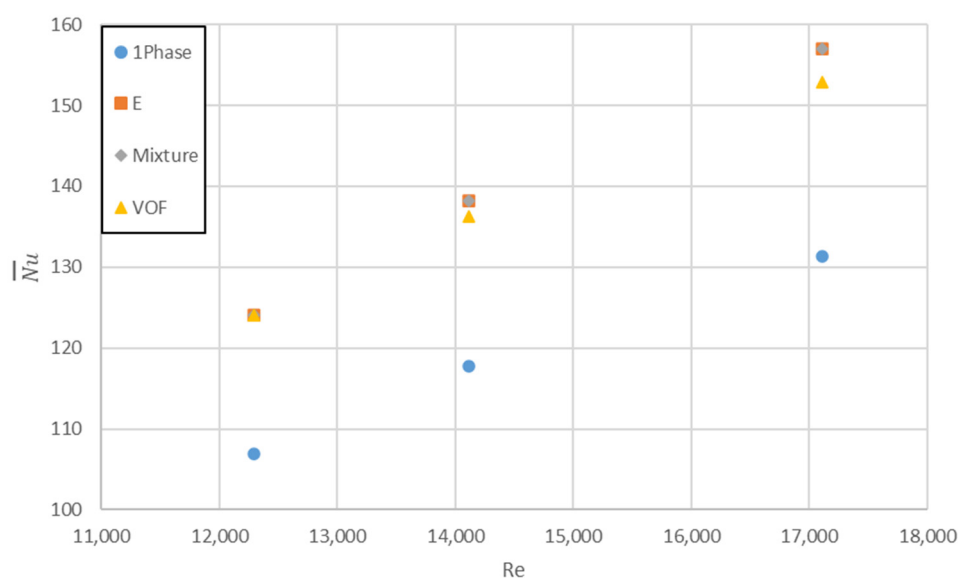


**Figure 3.**  $\overline{Nu}$ - $Re$  relationship for water- $Al_2O_3$  (1%) nanofluid—data source [29].

Alvarino et al. [30] studied the effect of the Brownian motion and thermophoretic diffusion on heat transfer during laminar flow of nanofluid in uniformly heated tube. A single-phase approach was considered. It was established that the heat transfer enhancement by the nanofluid had to be attributed to its thermophysical properties rather than to another transport mechanism. Tahir and Mital [31] investigated a developing laminar flow of nanofluid in a uniformly heated tube by use of discrete phase modeling (DPM) and a Euler-Lagrangian approach. The fluid was treated as a continuous medium and the flow field was solved based on Navier-Stokes equations. The nanoparticles were individually tracked in a Lagrangian reference frame and their trajectories were determined using particle force balance. Using this approach, a good match was obtained between the numerical model and the experimental results reported in the literature. Based on statistical analysis, it was established that almost all of the variation in the HTC can be explained due to changes in the three independent variables. The  $Re$  number is the most significant variable impacting the HTC, while NPC is the least significant. The HTC linearly increases with both  $Re$  number and NPC, but shows non-linear parabolic decrease with an increase in particle size. In addition, the three variables only weakly interact with each other in terms of their impact on the average HTC. Balla et al. [32] analyzed the effect of NPC on

heat transfer and PD of nanofluids during laminar flow in a uniformly heated tube. It was established that the Nu number, HTC, and PD strongly increase with the increase of NPC. In [33] Bayat and Nikseresht studied influence of temperature and NPC on heat transfer and PD during turbulent flow of nanofluid in a uniformly heated tube. A single-phase approach with temperature and nanoparticle concentration dependent properties of nanofluids was applied. It was concluded that application of nanofluids in a turbulent flow regime results in substantially higher PD and pumping power (PP) compared to base fluid for the same Re number. Moraveji and Esmaeili [34] investigated the laminar flow of nanofluid in uniformly heated tube. A single-phase model and discrete phase approach with selected properties of nanofluids was calculated as temperature dependent. The HTC increase with NPC increase was observed. There was no significant difference between the results for the single-phase model and discrete model. Davarnejad et al. [35] studied the influence of NPC on heat transfer during the laminar flow of nanofluids. A single-phase approach with properties of nanofluids calculated for the mean temperature was applied. Constant heat transfer coefficient was assumed as a boundary condition at the tube wall. It was shown that HTC increases with NPC and Pe number increase. In [36] Davarnejad et al. analyzed the influence of nanoparticle size and NPC on heat transfer during laminar flow in a uniformly heated tube. A single-phase approach with properties of nanofluids calculated for the mean temperature was applied. It was shown that HTC increases with nanoparticle size decrease. Kayaci et al. [37] studied the influence of NPC on heat transfer during the turbulent flow of nanofluids in an isothermally heated tube. A single-phase approach with the  $k-\varepsilon$  turbulence model was applied. A slight increase of HTC with NPC increase was observed. Hejazian and Moraveji [38] conducted an investigation on turbulent nanofluid flow inside an isothermal tube. A single-phase approach and mixture model with the  $k-\varepsilon$  turbulence model were tested. It was established that Nu number increases with NPC increase. Second, the mixture model better fits experimental data than the single-phase approach. Göktepe et al. [39] tested the ability of the single-phase model and two-phase models (Eulerian–Eulerian and Eulerian–mixture) to reproduce published experimental HTC and friction factors (FF) for laminar flow at the developing region of uniformly heated tube. It was established that two-phase models predict HTC and FF more accurately than single-phase models. Among single-phase models, the dispersion model that uses velocity gradient to define dispersion conductivity, was found to be more effective compared to the other. Moreover, the Eulerian–Eulerian model is recommended for cases when no prior experimental data is available. Figure 4 shows a comparison of numerical calculations by the use of two single-phase models with differently assumed dispersion conductivity (1PhaseD1, 1PhaseD2) and two two-phase models, namely Eulerian–mixture model (E–Mixture) and Eulerian–Eulerian model (E–E).

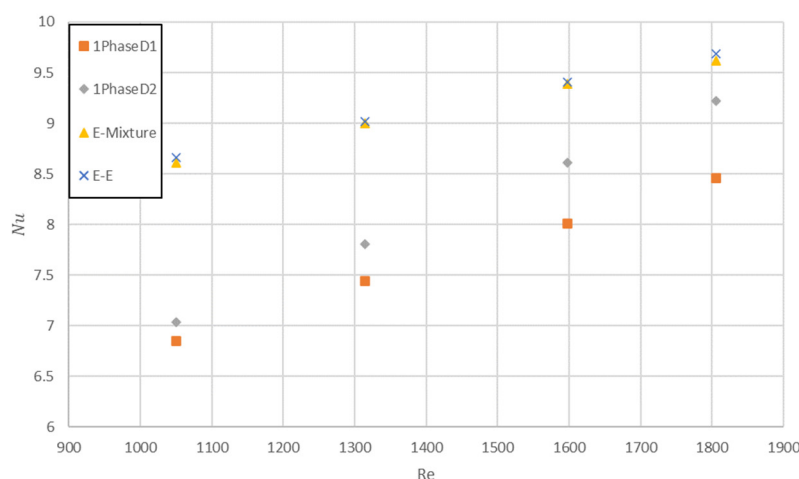
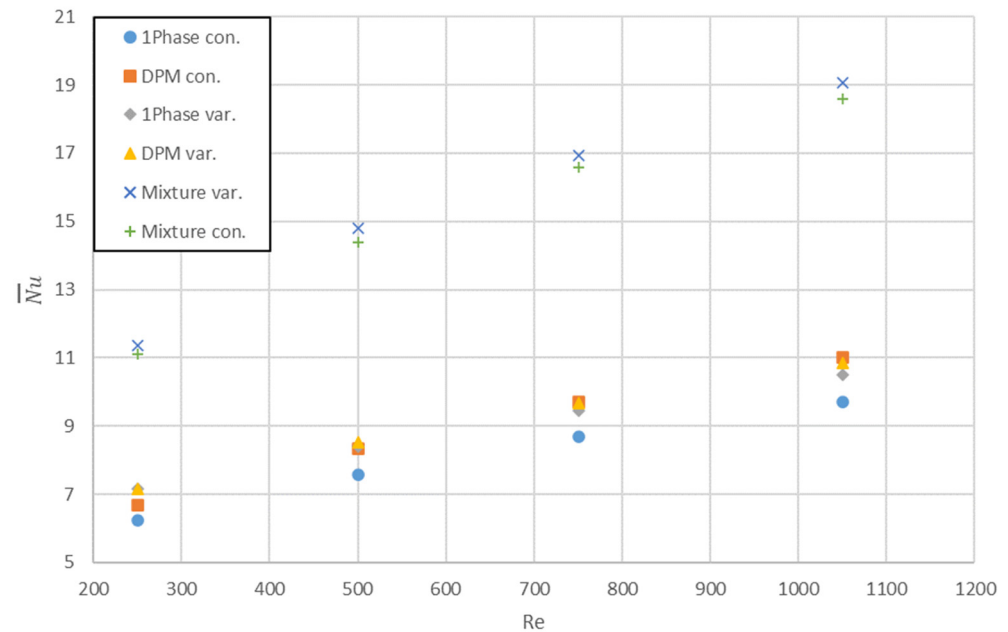


Figure 4. Nu-Re relationship for water–Al<sub>2</sub>O<sub>3</sub> (1.6%) nanofluid and  $x/D = 116$ —data source [39].



Saha and Paul [40] studied the influence of nanoparticle size, NPC, and Brownian motion on heat transfer and WSS during the turbulent flow of a nanofluid inside a uniformly heated tube. The single-phase approach with  $k-\epsilon$  turbulence model was applied to solve governing equations. It was established that heat transfer is more affected by the diameter of nanoparticles and Brownian motion than the thermal conductivity of a nanofluid. Bianco et al. [41] studied the influence of NPC on the turbulent flow of nanofluids in tubes with a constant wall temperature. A mixture model of nanofluid with  $k-\epsilon$  turbulence model was adopted. Although Nu number increases with NPC increase, PD increases more, so the application of nanofluids is questionable. In [42] Saha and Paul applied a Eulerian–Eulerian multi-phase mixture model to analyze the turbulent flow of nanofluids in a uniformly heated tube. It was found that heat transfer performance determined by the multi-phase mixture model is better than the single-phase model [40]. Aghaei et al. [43] simulated the effect of NPC and nanoparticle diameter on the turbulent behavior of nanofluids during flow in tube with a constant temperature. A mixture model with  $k-\epsilon$  turbulence model was applied. It was shown that there is an optimum value for the Nu number depending on the NPC. Moreover, the increase of nanoparticle diameter results in a Nu number decrease. Minea [44] studied the turbulent flow of nanofluids in a long tube with an isothermal entrance zone and a uniformly heated section of the developed region. A single-phase approach with the  $k-\epsilon$  turbulence model has been applied. It was established that HTC increases monotonically with NPC. Although PP increases with NPC in three case studies, the opposite trend was determined in one case study. Nasiri-lohesara [45] stated that the enhancement of heat transfer with NPC increased during turbulent nanofluid flow inside a tube-in-tube heat exchanger. However, the HTC rate of increase was less than the WSS increase. A mixture model of nanofluid with  $k-\epsilon$  turbulence model was applied. Ehsan and Noor [46] established a substantial enhancement of heat transfer during the flow of nanofluid in a rough tube compared to a smooth tube. Moreover, it was shown that there is an optimum value of NPC for which the PP is less than the base liquid. A single-phase approach with an SST  $k-\omega$  turbulence model was applied. Mahdavi et al. [47] tested different turbulence models by use of a mixture model and DPM implemented in ANSYS-FLUENT code to study the behavior of nanofluids flow in uniformly heated tubes of various lengths and diameters. According to Mahdavi et al. the realizable and standard  $k-\epsilon$  models provided the same results in most of the simulations. The Reynolds stress model (RSM) overestimates PD compared with the other  $k-\epsilon$  models, while the re-normalization group (RNG) model overestimates HTC. The DPM model is recommended for the discussed cases, however, as it was stressed, the number of particles plays a key role in the simulations. Purohit et al. [48] studied the laminar flow of nanofluids inside a uniformly heated tube by the use of the single-phase approach. It was established that HTC and WSS increase monotonically with NPC increase. Jahanbin [49] used single-phase and dispersion models to study the laminar flow of nanofluids in a uniformly heated tube. Moreover, in both models, constant and temperature dependent properties of nanofluids were tested. It was established that dispersion model shows better agreement with the existing experimental data than the single-phase model. Elahmer et al. [50] studied the laminar flow of nanofluids in a tube with a wall loaded with constant or periodic heat flux. A single-phase approach was applied. Regardless of the method of heating the wall of the tube, HTC increased with NPC increase. Albojamal and Vafai [51] conducted simulations of laminar nanofluid flow in a tube with a uniformly heated wall. A single-phase model, the Lagrangian–Eulerian model (DPM), and the mixture model were adopted with both constant and temperature-dependent properties of nanofluids. It was observed that the DPM model overestimated the HTC. The mixture model predicted unreasonable heat transfer enhancement, particularly for high NPC. The single-phase model displayed a very good agreement with the experimental data. It was established that HTC increases with NPC and Re number increase, but it is punished by PD and WSS increases. Finally, it was concluded that the proposed single-phase model reproduces the experimental data with sufficient accuracy and there is no need for two-phase models. In Figure 5, results of

numerical calculations by the use of the single-phase (1Phase) approach and two two-phase models, namely DPM and mixture, with constant (con.) and variable (var.) thermophysical properties of nanofluid, are shown.



**Figure 5.**  $\overline{Nu}$ - $Re$  relationship for water- $Al_2O_3$  (4%) nanofluid—data source [51].

Rashidi et al. [52] used single-phase model, VOF model, mixture model, and Eulerian model to study entropy generation during turbulent flow of nanofluids in a uniformly heated tube. The  $k-\epsilon$  turbulence model was applied. It was established that the entropy generation were very similar for the single-phase and mixture models. Rabby et al. [53] studied the laminar flow of nanofluids in a uniformly heated tube by use of the single-phase approach. It was determined that a substantial HTC increase is accompanied by a small FF increase with NPC increase. Boertz et al. [54] conducted a numerical simulation of turbulent nanofluid flow in a tube with a uniformly heated wall by use of the single-phase approach with an SST  $k-\omega$  turbulence model. It was established that the Nu number increases significantly with NPC increase; however, FF and PP also increase. Kristiawan et al. [54] used a Eulerian approach to study laminar and turbulent flows of nanofluid in a uniformly heated tube. For turbulent flow, the  $k-\epsilon$  turbulence model was applied. It was determined that the HTC of nanofluid increases considerably compared to the base liquid in both laminar and turbulent flow. According to [55] the Eulerian approach should be applied for nanofluids with higher NPC. Sajjad et al. [56] studied the laminar flow of nanofluid in a uniformly heated tube by use of the single-phase model with temperature-dependent properties. It was established that an increase in local HTC is more distinct in the entrance region. Moreover, the addition of nanoparticles results in a higher average HTC, but is punished with higher PD with NPC increase. Minea et al. [57] conducted an inter-comparative study on the 3D laminar flow of nanofluids in uniformly heated tube by the use of four single-phase models and two mixture models. It was established that numerical results overpredict the experimental data and the two-phase approach is more appropriate to simulate nanofluid behavior. Onyiriuka and Ikponmwoba [58] applied a mixture model to study the laminar flow of nanofluids inside a uniformly heated tube. Constant properties of the tested bio-nanofluid were assumed. It was established that HTC increases with NPC increase. Jamali and Toghraie [59] studied the transition from laminar to turbulent flow of nanofluid in an isothermal tube by use of the single-phase approach. The effect of the nanoparticle diameter, NPC, and type of nanoparticles was studied. It was established that the addition of nanoparticles does not affect the onset of transition. Fadodun et al. [60] studied the turbulent flow of nanofluids in a uniformly

heated tube by the use of the single-phase approach. The  $k-\epsilon$  turbulence model was applied with temperature-dependent properties of nanofluid. Heat transfer enhancement with simultaneous PD increase was observed for NPC increase. Saeed and Al-Dulaimi [61] applied the single-phase approach and four different sets of thermophysical properties to study the laminar flow of a nanofluid in a uniformly heated tube. It was determined that both temperature-dependent and temperature-independent models of thermophysical properties of nanofluids can correctly reproduce the behavior of nanofluids during laminar flow. Uribe et al. [62] studied the 3D laminar and turbulent flows of nanofluid in a uniformly heated tube by the use of the single-phase approach. It was established that HTC increases with NPC increase, while thermal boundary thickness decreases with NPC increase. It was stated that there is no need to apply two-phase models to describe nanofluid behavior. Taskesen et al. [63] studied the influence of channel geometry (circular, square, triangular, and rectangular) on the thermo-hydraulic behavior of nanofluid during laminar flow. A single-phase model with temperature-dependent properties was applied. Heat transfer enhancement was observed with an NPC increase, and a circular cross-section was superior over other geometries. Yildiz and Aktürk [64] used a single-phase approach to study the 3D turbulent flow of a nanofluid inside a uniformly heated tube. The standard  $k-\epsilon$  turbulence model with temperature-dependent properties was applied. A substantial increase of Nu number and HTC was recorded. However, FF increases markedly with NPC increase. In Tables 1 and 2 details of the studies in which the single-phase approach and two-phase models were applied are presented, respectively.

**Table 1.** Numerical studies dealing with single-phase approach.

| Executors                        | Approach   | Nanofluid   | Geometry/BCon   | Re Number/<br>NPC  | Result   |
|----------------------------------|--|---|---|--|--|
| Maïga et al. [12]                | Single-phase   | water- $\gamma$ Al <sub>2</sub> O <sub>3</sub>  | D = 10 mm<br>L = 1000 mm<br>q = const.  | $10^4 < Re < 5 \times 10^4$<br>$0 < \varphi_v [\%] < 10$                               | AHTCE (60%)<br>AWSSI (180%)  |
| Maïga et al. [13]                | Single-phase   | water- $\gamma$ Al <sub>2</sub> O <sub>3</sub><br>EG- $\gamma$ Al <sub>2</sub> O <sub>3</sub>   | D = 10 mm<br>L = 1000 mm<br>q = const.<br>$t_w = \text{const.}$   | $250 < Re < 10^3$<br>(Water)<br>$6.31 < Re < 631$<br>(EG)<br>$0 < \varphi_v [\%] < 10$ | AHTCE (180%)<br>AWSSI (1207%) for<br>EG- $\gamma$ Al <sub>2</sub> O <sub>3</sub> |
| Maïga et al. [14]                | Single-phase   | water- $\gamma$ Al <sub>2</sub> O <sub>3</sub>  | D = 10 mm<br>L = 1000 mm<br>q = const.  | $10^4 < Re < 5 \times 10^5$<br>$0 < \varphi_v [\%] < 10$                               | FDHTCE (75%)<br>FDWSSI (581%)  |
| Heris et al. [15]                | Dispersion model   | water-Al <sub>2</sub> O <sub>3</sub><br>water-CuO<br>water-Cu                                   | D = 5 mm<br>L = 1000 mm<br>$t_w = \text{const.}$  | $2500 < P e < 6500$<br>$0.5 < \varphi_v [\%] < 5$                                      | ANuNE (100%)   |
| Namburu et al. [20]              | Single-phase   | EG-water (60:40)/<br>CuO, Al <sub>2</sub> O <sub>3</sub> , SiO <sub>2</sub>                     | D = 10 mm<br>L = 800 mm<br>q = const.   | $10^4 < Re < 10^5$<br>$0 < \varphi_v [\%] < 6$   | AHTCE (75%)  |
| Mokmeli and<br>Saffar-Avval [23] | <ul style="list-style-type: none"> <li>• Single-phase</li> <li>• Dispersion model</li> </ul> | water- $\gamma$ Al <sub>2</sub> O <sub>3</sub><br>ATF-G<br>water-Al <sub>2</sub> O <sub>3</sub> | D = 4.5 mm<br>L = 970 mm<br>D = 4.57 mm<br>L = 457 mm<br>D = 6 mm<br>L = 1000 mm<br>q = const.<br>$t_w = \text{const.}$ | $19.67 < Re < 1810$<br>$1 < \varphi_m [\%] < 1.6$                                      | Single-phase<br>model → NuND<br>(31%)<br>Dispersion model<br>→ NuNE (15%)        |



Table 1. Cont.

| Executors                       | Approach   | Nanofluid   | Geometry/BCon   | Re Number/<br>NPC  | Result   |
|---------------------------------|--|---|---|--|--|
| Ebrahimnia-Bajestan et al. [24] | Single-phase   | EG-water (60:40) water;<br>Al <sub>2</sub> O <sub>3</sub> , CuO, CNT, TNT   | D = 4.57 mm<br>L = 2000 mm<br>q = const.              | 500 < Re < 1460<br>0 < φ <sub>v</sub> [%] < 6                            | HTCE (22%)<br>PDI (3880%)                        |
| Moraveji et al. [25]            | Single-phase   | water–Al <sub>2</sub> O <sub>3</sub>  | D = 4.75 mm<br>L = 970 mm<br>q = const.               | 500 < Re < 2500<br>1 < φ <sub>m</sub> [%] < 6                            | HTCE (20%)                                       |
| Bayat and Nikseresht [27]       | Single-phase   | Water–Al <sub>2</sub> O <sub>3</sub><br>EG–Al <sub>2</sub> O <sub>3</sub><br>EG–water (60:40)/Al <sub>2</sub> O <sub>3</sub><br>EG–water (30:70)/Al <sub>2</sub> O <sub>3</sub> | D = 4.57 mm<br>L = 2000 mm<br>q = const.              | 100 < Re < 2000<br>0 < φ <sub>v</sub> [%] < 9                            | AHTCE (42%)<br>ASSI (500%)                       |
| Alvarino et al. [30]            | Single-phase   | water–Al <sub>2</sub> O <sub>3</sub>  | D = 4.5 mm<br>L = 970 mm<br>q = const.                | 750 < Re < 1750<br>0 < φ <sub>v</sub> [%] < 1.6                          | HTCE (12%)                                       |
| Balla et al. [32]               | Single-phase   | water–Al <sub>2</sub> O <sub>3</sub><br>water–CuO<br>water–TiO <sub>2</sub>   | D = 10 mm<br>L = 2000 mm<br>q = const.                | 100 < Re < 1000<br>0 < φ <sub>v</sub> [%] < 4                            | HTCE (25%)                                       |
| Bayat and Nikseresht [33]       | Single-phase   | EG–water (60:40)/Al <sub>2</sub> O <sub>3</sub>   | D = 10 mm<br>L = 1000 mm<br>q = const.                | 10 <sup>4</sup> < Re < 10 <sup>5</sup><br>1 < φ <sub>v</sub> [%] < 10    | AHTCE (70%)<br>PDI (230%)                        |
| Davarnejad et al. [35]          | Single-phase   | water–Al <sub>2</sub> O <sub>3</sub>  | D = 6 mm<br>L = 1000 mm<br>h = const.                 | 700 < Re < 2050<br>0 < φ <sub>v</sub> [%] < 2.5                          | HTCE (25%)                                       |
| Davarnejad et al. [36]          | Single-phase   | water–Al <sub>2</sub> O <sub>3</sub>  | D = 6 mm<br>L = 1000 mm<br>q = const.                 | 700 < Re < 2050<br>0 < φ <sub>v</sub> [%] < 2.5                          | AHTCE (7%)                                       |
| Kayaci et al. [37]              | Single phase   | water–TiO <sub>2</sub>  | D = 8.13 mm<br>L = 1500 mm<br>t <sub>w</sub> = const. | 7233 < Re < 13,340<br>0.2 < φ <sub>v</sub> [%] < 1                       | HTCE (3%)<br>PDI (6.5%)<br>FFI (5%)<br>WSSI (5%) |
| Saha and Paul [40]              | Single-phase   | water–Al <sub>2</sub> O <sub>3</sub><br>water–TiO <sub>2</sub>  | D = 19 mm<br>L = 1000 mm<br>q = const.                | 10 <sup>4</sup> < Re < 10 <sup>5</sup><br>0 < φ <sub>v</sub> [%] < 6     | ANuNE (60%)<br>AWSSI (1363%)                     |
| Minea [44]                      | Single-phase   | water–Al <sub>2</sub> O <sub>3</sub>  | D = 12 mm<br>L = 8760 mm<br>q = const.                | 10 <sup>7</sup> < Re < 3 × 10 <sup>7</sup><br>0 < φ <sub>v</sub> [%] < 4 | HTCE (26%)<br>PPI (16%)<br>PPD (10%)             |
| Ehsan and Noor [46]             | Single-phase   | water–Al <sub>2</sub> O <sub>3</sub>  | D = 3 mm<br>L = 300 mm<br>q = const.                  | 10 <sup>4</sup> < Re < 3 × 10 <sup>4</sup><br>1–5%vol.                   | HTCE (39%)<br>PPI (203%)                         |
| Purohit et al. [48]             | Single-phase   | water–Al <sub>2</sub> O <sub>3</sub><br>water–ZrO <sub>2</sub><br>water–TiO <sub>2</sub>  | L = 1000 mm<br>q = const.                             | 1150 < Re < 1900<br>0.5 < φ <sub>v</sub> [%] < 2                         | HTCE (18%)<br>WSSI (3%)                          |
| Jahanbin [49]                   | <ul style="list-style-type: none"> <li>• Single phase</li> <li>• Dispersion model</li> </ul> | water–Al <sub>2</sub> O <sub>3</sub>  | D = 10 mm<br>L = 1000 mm<br>q = const.                | 250 < Re < 1250<br>1 < φ <sub>m</sub> [%] < 4                            | HTCE (49%)<br>WSSI (156%)                        |

Table 1. Cont.

| Executors                 | Approach     | Nanofluid   | Geometry/BCon   | Re Number/<br>NPC   | Result                                 |
|---------------------------|--------------|---|---|---|--|
| Elahmer et al. [50]       | Single-phase | EG-CNT<br>EG-CNT-Ag   | D = 10 mm<br>q = const.<br>q-periodic                 | Pe = 10 <sup>3</sup> and Pe = 2 × 10 <sup>3</sup><br>0 < φ <sub>v,CNT</sub> [%] < 10<br>φ <sub>v,Ag</sub> [%] = 1 | HTCE (67%)                             |
| Rabby et al. [53]         | Single-phase | water–Al <sub>2</sub> O <sub>3</sub>  | D = 5 mm<br>L = 750 mm<br>q = const.                  | 100 < Re < 1400<br>1 < φ <sub>v</sub> [%] < 5   | HTCE (32%)<br>NuNE (15%)<br>FFI (2%)   |
| Boertz et al. [54]        | Single-phase | EG/W (60:40)<br>wt–SiO <sub>2</sub>   | D = 3.14 mm<br>L = 1168 mm<br>q = const.              | 6 × 10 <sup>3</sup> < Re < 1.2 × 10 <sup>4</sup><br>2 < φ <sub>v</sub> [%] < 10                                   | ANuNE (15%)<br>FFI (13%)               |
| Sajjad et al. [56]        | Single-phase | EG/W (40:60)<br>wt–GO   | D = 4.5 mm<br>L = 2000 mm<br>q = const.               | 400 < Re < 2000<br>0.01 < φ <sub>m</sub> [%] < 0.1  | HTCE (13%)<br>PDI (112%)               |
| Jamali and Toghraie [59]  | Single-phase | water–Al <sub>2</sub> O <sub>3</sub><br>water–CuO   | D = 8.14 mm<br>L = 7400 mm<br>t <sub>w</sub> = const. | 500 < Re < 13,000<br>0 < φ <sub>v</sub> [%] < 4   | AHTCE (14%)                            |
| Fadodun et al. [60]       | Single-phase | water–Al <sub>2</sub> O <sub>3</sub>  | D = 20 mm<br>L = 2000 mm<br>q = const.                | 5000 < Re < 15,000<br>1 < φ <sub>v</sub> [%] < 5  | AHTCE<br>PDI<br>(values not specified) |
| Saeed and Al-Dulaimi [61] | Single-phase | water–TiO <sub>2</sub>  | D = 4 mm<br>L = 2000 mm<br>q = const.                 | Re = 900<br>0.6 < φ <sub>v</sub> [%] < 1.18   | HTCE (28%)                             |
| Uribe et al. [62]         | Single-phase | water–CuO<br>water–Al <sub>2</sub> O <sub>3</sub><br>water–Fe <sub>2</sub> O <sub>3</sub> | D = 25.4 mm<br>L = 400 mm<br>q = const.               | 10 <sup>3</sup> < Re < 11 × 10 <sup>3</sup><br>0.01 < φ <sub>v</sub> [%] < 0.05                                   | HTCE (18%)                             |
| Taskesen et al. [63]      | Single-phase | water–Fe <sub>3</sub> O <sub>4</sub>  | D = 16 mm<br>L = 1500 mm<br>q = const.                | 500 < Re < 2000<br>1 < φ <sub>v</sub> [%] < 5   | ANuNE (4%)<br>PDI (50%)                |
| Yildiz and Aktürk [64]    | Single-phase | water–Al <sub>2</sub> O <sub>3</sub>  | D = 17 mm<br>L = 350 mm<br>q = const.                 | 4000 < Re < 9000<br>1 < φ <sub>v</sub> [%] < 4  | HTCE (53%)<br>ANuNE (32%)<br>FFI (41%) |

Table 2. Numerical studies dealing with two-phase approach.

| Executors              | Approach   | Nanofluid                             | Geometry/BCon                          | Re Number/<br>NPC                                       | Result                     |
|------------------------|--|---------------------------------------|--|---|----------------------------|
| Behzadmehr et al. [16] | <ul style="list-style-type: none"> <li>Mixture model</li> <li>Single-phase</li> </ul>  | water–Cu                              | 0 ≤ x/D ≤ 100<br>q = const.            | 10,515 < Re < 22,540<br>φ <sub>v</sub> = 1%             | ANuNE (15%)<br>FC ≈ const. |
| Bianco et al. [17]     | <ul style="list-style-type: none"> <li>Discrete-phase</li> <li>Single-phase</li> </ul> | water–Al <sub>2</sub> O <sub>3</sub>  | D = 10 mm<br>L = 1000 mm<br>q = const. | Re = 1050<br>1 < φ <sub>v</sub> [%] < 4                 | HTCE (20%)<br>WSSI (54%)   |
| Bianco et al. [18]     | <ul style="list-style-type: none"> <li>Discrete-phase</li> <li>Single-phase</li> </ul> | water–γAl <sub>2</sub> O <sub>3</sub> | D = 10 mm<br>L = 1000 mm<br>q = const. | 250 < Re < 1050<br>1 < φ <sub>v</sub> [%] < 4           | NuNE(17%)<br>WSSI (101%)   |
| He et al. [19]         | <ul style="list-style-type: none"> <li>Euler-DPM</li> <li>Single-phase</li> </ul>      | water–TiO <sub>2</sub>                | D = 4 mm<br>L = 2000 mm<br>q = const.  | Re = 900, Re = 1500<br>0.24 < φ <sub>v</sub> [%] < 1.18 | HTCE (14%)                 |

Table 2. Cont.

| Executors                  | Approach  | Nanofluid  | Geometry/BCon   | Re Number/<br>NPC   | Result  |
|----------------------------|---|--|---|---|---|
| Fard et al. [21]           | <ul style="list-style-type: none"> <li>Two-phase (CFX code)</li> <li>Single-phase</li> </ul>  | water–Cu<br>water–CuO<br>water–Al <sub>2</sub> O <sub>3</sub>  | D = 6 mm<br>L = 1000 mm<br>t <sub>w</sub> = const.  | 700 < Re < 2050<br>0 < φ <sub>v</sub> [%] < 3   | AHTCE (54%) for CuO   |
| Lotfi et al. [22]          | <ul style="list-style-type: none"> <li>Mixture model</li> <li>Eulerian model</li> <li>Single-phase</li> </ul>                                       | water–Al <sub>2</sub> O <sub>3</sub>   | D = 45 mm<br>L = 970 mm<br>q = const.   | 700 < Re < 1800<br>2 < φ <sub>v</sub> [%] < 7   | NuND (46%)  |
| Bianco et al. [26]         | <ul style="list-style-type: none"> <li>Mixture model</li> <li>Single-phase</li> </ul>   | water–Al <sub>2</sub> O <sub>3</sub>   | D = 10 mm<br>L = 1000 mm<br>q = const.  | 10 <sup>4</sup> < Re < 10 <sup>5</sup><br>0 ≤ φ <sub>m</sub> [%] < 6                    | HTCE (20%)  |
| Akbari [28]                | <ul style="list-style-type: none"> <li>VOF</li> <li>Mixture model</li> <li>Eulerian model</li> <li>Single-phase</li> </ul>                          | water–Al <sub>2</sub> O <sub>3</sub>   | D = 4.5 mm<br>L = 1500 mm<br>q = const  | Re = 1050 and Re = 1600<br>φ <sub>v</sub> [%] < 2                                       | E model → AHTCD (15%)<br>Single-phase model → AHTCD (44%)   |
| Akbari [29]                | <ul style="list-style-type: none"> <li>VOF</li> <li>Mixture model</li> <li>Eulerian model</li> <li>Single-phase</li> </ul>                          | water–Al <sub>2</sub> O <sub>3</sub><br>water–Cu   | D = 19 mm<br>L = 1500 mm<br>D = 10 mm<br>L = 800 mm<br>q = const.   | 9.7 × 10 <sup>4</sup> < Re < 17.7 × 10 <sup>4</sup><br>1 < φ <sub>v</sub> [%] < 2       | ANuNE (213%) for VOF<br>and Mixture model<br>ANuNE (0%) for<br>single-phase model<br>FFI (13%)  |
| Tahir and Mital [31]       | Discrete-phase model  | water–Al <sub>2</sub> O <sub>3</sub>   | D = 10 mm<br>L = 1000 mm<br>q = const.  | 250 < Re < 1250<br>1 < φ <sub>v</sub> [%] < 4   | AHTCE (25%)   |
| Moraveji and Esmaili [34]  | <ul style="list-style-type: none"> <li>Discrete-phase</li> <li>Single-phase</li> </ul>  | water–Al <sub>2</sub> O <sub>3</sub>   | D = 10 mm<br>L = 1000 mm<br>q = const.  | 250 < Re < 1050<br>0 < φ <sub>v</sub> [%] < 4   | AHTCE (32%)   |
| Hejazian and Moraveji [38] | <ul style="list-style-type: none"> <li>Mixture model</li> <li>Single-phase</li> </ul>   | water–TiO <sub>2</sub>   | D = 5 mm<br>L = 1200 mm<br>t <sub>w</sub> = const.  | 4.8 × 10 <sup>3</sup> < Re < 30.5 × 10 <sup>3</sup><br>0.05 < φ <sub>v</sub> [%] < 0.25 | ANuNE(52%)  |
| Göktepe et al. [39]        | <ul style="list-style-type: none"> <li>Eulerian–mixture model</li> <li>Eulerian–Eulerian</li> <li>Single-phase</li> <li>Dispersion model</li> </ul> | water–Al <sub>2</sub> O <sub>3</sub>   | D = 4.5 mm<br>L = 2000 mm<br>q = const.   | 1050 < Re < 1810<br>0.6 < φ <sub>v</sub> [%] < 1.6                                      | HTCD or HTCE<br>depending on the model<br>and (x/D) value<br>FFI (2%)   |
| Bianco et al. [41]         | Mixture model   | water–Al <sub>2</sub> O <sub>3</sub>   | D = 10 mm<br>L = 1000 mm<br>t <sub>w</sub> = const.   | 20,103 < Re < 105<br>0 < φ <sub>v</sub> [%] < 4   | HFI (33%)<br>PPI (450%)   |
| Saha and Paul [42]         | Eulerian–Eulerian model   | water–Al <sub>2</sub> O <sub>3</sub><br>water–TiO <sub>2</sub>   | D = 19 mm<br>L = 1000 mm<br>q = const.  | 10 <sup>4</sup> < Re < 10 <sup>5</sup><br>0 < φ <sub>v</sub> [%] < 6                    | NuNE (62%)<br>WSSI (1335%)<br>FCI   |
| Aghaei et al. [43]         | Mixture model   | water–Al <sub>2</sub> O <sub>3</sub>   | D = 20 mm<br>L = 1000 mm<br>t <sub>w</sub> = const.   | 10 <sup>4</sup> < Re < 10 <sup>5</sup><br>0 < φ <sub>v</sub> [%] < 4                    | NuN ≈ const. for<br>φ <sub>v</sub> ≤ 0.02<br>NuND (4%) for φ <sub>v</sub> ≤ 0.02<br>PDI (17%)<br>FCI (5%)   |
| Nasiri-lohesara [45]       | Mixture model   | water–γAl <sub>2</sub> O <sub>3</sub>  | D = 10 mm<br>L = 650 mm   | 2 × 10 <sup>4</sup> < Re < 5 × 10 <sup>4</sup><br>0 < φ <sub>v</sub> [%] < 6            | HTCE (32%)<br>WSSI (203%)   |
| Mahdavi et al. [47]        | <ul style="list-style-type: none"> <li>Mixture model</li> <li>Discrete-phase</li> </ul>   | water–Al <sub>2</sub> O <sub>3</sub><br>water–ZrO <sub>2</sub><br>water–TiO <sub>2</sub><br>water–SiO <sub>2</sub> | D = 10.26 mm<br>L = 3000 mm<br>D = 3.5 mm<br>L = 600 mm<br>D = 9.4 mm<br>L = 3000 mm<br>D = 10.6 mm<br>L = 1500 mm<br>q = const., q = 0 | 3500 < Re < 63,000<br>0.2 < φ <sub>v</sub> [%] < 3.6                                    | <b>Mixture model</b> <ul style="list-style-type: none"> <li>k-εRNG–overpredicts ExHTC (12%)</li> <li>k-εS &amp; R and RSM fit ExHTC</li> </ul> <b>DPM</b><br>k-εRNG, k-εS&R, and RSM overpredict ExHTC (1.8%) |

Table 2. Cont.

| Executors                     | Approach   | Nanofluid                            | Geometry/BCon                            | Re Number/<br>NPC  | Result  |
|-------------------------------|--|--------------------------------------|--|--|---|
| Albojamal and Vafai [51]      | <ul style="list-style-type: none"> <li>Mixture model</li> <li>Discrete-Phase</li> <li>Single-phase</li> </ul>              | water-Al <sub>2</sub> O <sub>3</sub> | D = 10 mm<br>L = 1000 mm<br>q = const.   | 250 < Re < 1460<br>1 < φ <sub>v</sub> [%] < 4  | HTCE: <ul style="list-style-type: none"> <li>Single-phase (19%)</li> <li>DPM (23%)</li> <li>Mixture (90%)</li> </ul> WSSI: <ul style="list-style-type: none"> <li>Single-phase (103%)</li> <li>DPM (184%)</li> <li>Mixture (80%)</li> </ul> |
| Rashidi et al. [52]           | <ul style="list-style-type: none"> <li>VOF</li> <li>Mixture model</li> <li>Eulerian model</li> <li>Single-phase</li> </ul> | water-TiO <sub>2</sub>               | D = 8.13 mm<br>L = 1500 mm<br>q = const. | 9 × 10 <sup>3</sup> < Re < 21 × 10 <sup>3</sup>  | NHTC fits ExHTC   |
| Kristiawan et al. [55]        | Eulerian model   | water-TiO <sub>2</sub>               | D = 5 mm<br>L = 2000 mm<br>q = const.    | 500 < Re < 1200<br>4 × 10 <sup>3</sup> < Re < 14 × 10 <sup>3</sup><br>0.24 < φ <sub>v</sub> [%] < 1.18 | HTCE: <ul style="list-style-type: none"> <li>Laminar (20%)</li> <li>turbulent (22%)</li> </ul>  |
| Minea et al. [57]             | <ul style="list-style-type: none"> <li>Mixture model</li> <li>Single-phase</li> </ul>                                      | water-TiO <sub>2</sub>               | D = 8 mm<br>L = 2000 mm<br>q = const.    | 1 < φ <sub>m</sub> [%] < 2.5   | TD (9%)   |
| Onyiriuka and Ikponmwoba [58] | Mixture model  | water-mango leaves                   | D = 19 mm<br>L = 1000 mm<br>q = const.   | 250 < Re < 1250<br>1 < φ <sub>v</sub> [%] < 3  | AHTCE (12%)   |

### 3. Heat Transfer Correlation Equations

As seen in Tables 3 and 4, a limited number of numerically developed correlation equations have been proposed. It is necessary to stress the very limited range of applications of the presented correlations.

Table 3. Correlation equations for laminar flow of nanofluids.

| Authors                   | Equation  | Range   |
|---------------------------|---|---|
| Maïga et al. [13]         | $\overline{Nu} = 0.086Re^{0.55}Pr^{0.5}q = \text{const.}$ $\overline{Nu} = 0.28Re^{0.35}Pr^{0.36}t_w = \text{const.}$ | Re < 1000<br>6 ≤ Pr ≤ 753<br>0 ≤ φ <sub>v</sub> [%] ≤ 10                                |
| Moraveji et al. [25]      | $Nu = 2.03\phi_v^{0.06}(x/D)^{-0.37}Re^{0.293}Pr^{0.6}$   | 500 < Re < 2300<br>6.8 < Pr < 11.97<br>1 < φ <sub>m</sub> [%] < 6                       |
| Tahir and Mital [31]      | $\bar{h} = 399 - 278(d_p/100) + 568(Re/1250) + 8(\phi_v/4) + 180(d_p/100)^2 - 100(Re/1250)^2 - 72(d_p/100)(Re/1250)$  | 250 < Re < 150<br>water-Al <sub>2</sub> O <sub>3</sub><br>1 < φ <sub>v</sub> [%] < 4    |
| Moraveji and Esmaili [34] | $Nu = 0.716Re^{0.314}.Pr^{0.6} \phi_v^{0.3}$  | 250 < Re < 1050<br>water-Al <sub>2</sub> O <sub>3</sub><br>0 < φ <sub>v</sub> [%] < 4   |
| Davarnajad et al. [35]    | $Nu = 0.18665\phi_v^{-0.00728}(x/D)^{0.1036}Re^{0.368718}Pr^{0.3992}$   | 700 < Re < 2050<br>water-Al <sub>2</sub> O <sub>3</sub><br>0 < φ <sub>v</sub> [%] < 2.5 |
| Taskesen et al. [63]      | $\overline{Nu} = 0.873747Re^{0.312881} + 4.98564\phi_v$   | 500 < Re < 2000<br>water-Fe <sub>3</sub> O <sub>4</sub><br>1 < φ <sub>v</sub> [%] < 5   |

**Table 4.** Correlation equations for turbulent flow of nanofluids.

| Authors                    | Equation   | Range   |
|----------------------------|--|---|
| Maïga et al. [13]          | $\overline{Nu} = 0.085Re^{0.71}Pr^{0.35}$  | $10^4 < Re < 5 \times 10^5$<br>$6.6 < Pr < 13.9$<br>$0 \leq \varphi_v [\%] \leq 10$   |
| Hejazian and Moraveji [38] | $\overline{Nu} = 0.00218Re^{1.0037}Pr^{0.5}(1 + \varphi_v)^{154.6471}$   | $4800 < Re < 30,500$<br>$5.5 < Pr < 5.59$<br>$0 \leq \varphi_v [\%] \leq 0.25$  |
| Saha and Paul [40]         | water–Al <sub>2</sub> O <sub>3</sub><br>$Nu = 0.01272Re^{0.85861}Pr^{0.42986}\left(\frac{d_f}{d_p}\right)^{-0.0017}$       | $10^4 < Re < 10^5$<br>$8.45 < Pr < 20.29$<br>$4\% < \varphi_v < 6\%$  |
|                            | water–TiO <sub>2</sub><br>$Nu = 0.01259Re^{0.85926}Pr^{0.43020}\left(\frac{d_f}{d_p}\right)^{-0.00068}$                    | $10 < d_p [nm] < 40$  |
| Saha and Paul [42]         | water–Al <sub>2</sub> O <sub>3</sub><br>$Nu = 0.01260Re^{0.85589}Pr^{0.44709}\left(\frac{d_f}{d_p}\right)^{-0.00176}$      | $10^4 < Re < 10^5$<br>$8.45 < Pr < 20.29$<br>$2\% < \varphi_v < 6\%$  |
|                            | water–TiO <sub>2</sub><br>$Nu = 0.01518Re^{0.84071}Pr^{0.44083}\left(\frac{d_f}{d_p}\right)^{-0.00534}$                    | $10 < d_p [nm] < 40$  |
| Aghaei et al. [43]         | $\overline{Nu} = 0.5277 \cdot 10^{-2}Re + 0.1625 \cdot 10^5 \varphi_v^2 + 0.3066 \cdot 10^3 \varphi_v + 0.3084 \cdot 10^2$ | $10^4 < Re < 10^5$<br>$Pr = 6.13$<br>$0.001 < \varphi_v < 0.04$<br>$25 < d_p [nm] < 100$  |
| Fadodun et al. [60]        | $\log_e \overline{Nu} = 4.23 + 0.13Re + 0.0063\varphi - 0.036T_{in}$   | $10^4 < Re < 10^5$<br>water–Al <sub>2</sub> O <sub>3</sub><br>$0.01 < \varphi_v < 0.05$<br>$20 < d_p [nm] < 100$<br>$290 < T [K] < 330$ |

#### 4. Conclusions

As shown in Table 1, a single-phase approach was used in the majority of works. The conclusions of the researchers who used single-phase models and two-phase models regarding the comparison of both approaches are different. Some of them [22,23] observed that the accuracy of the single-phase model is similar to the two-phase models. Others [11,12] indicate that the two-phase models more faithfully reproduce the results of experimental research than the single-phase approach. It was stressed that for nanofluids, the number of particles in the computational domain, even for a very small NPC, is very large. Therefore, due to limitations of the software abilities, the Lagrangian–Eulerian approach is extremely difficult to implement.

Several investigators [19,30,31,34,39,47,51,57] implemented mechanisms influencing convective heat transfer of nanofluids previously considered by Buongiorno [65]. According to [19,30], Brownian motion and thermophoresis have a negligible impact on heat transfer during the forced convection of nanofluids. Moreover, Albojamal and Vafai [51] demonstrated that the Brownian motion, thermophoresis, virtual mass, pressure gradient, and Saffman lift force do not significantly influence mean HTC. It was shown in [47] that gravity, virtual mass, pressure gradient, Brownian, and lift forces have no impact on mean flow field. As stated in [57], gravity force has to be included in all numerical models.

There is also no consensus among researchers regarding the assumption of constant or temperature-dependent thermophysical properties of nanofluids. In [33,34,61], a greater accuracy of the model using temperature-dependent thermophysical properties was observed, compared to the model where the thermophysical properties were constant.

Generally, the standard  $k$ - $\epsilon$  turbulence model was used to model turbulent flows of nanofluids [14,16,20,26,29,33,37,40,55,60,62]. Only a few studies used other models of turbulence [4–8].



Virtually all the results of numerical studies indicate the intensification of the heat transfer of nanofluids compared to base liquids, regardless of the type of flow (laminar or turbulent), although the results of the experimental studies are not so clear, e.g., [66–68].

There is also full agreement that the addition of nanoparticles increases flow resistance (PD, FF, and WSS).

Many researchers point to the need to intensify research on the thermophysical properties of nanofluids, as they determine the accuracy of the single-phase model first of all. In this context, however, one must bear in mind the limitations of experimental research [69].

The heat transfer correlations proposed in the literature have a very limited range of applicability. No numerically developed correlation for determination of the friction factor of nanofluids flowing inside a horizontal smooth tube has been presented.

Future works should concern a benchmark solution for laminar and turbulent flow of nanofluids similar to that of Buongiorno et al. in relation to thermal conductivity [70]. It is necessary to conduct a comparative study of the influence of divergent thermophysical properties of base liquids on the final results concerning the influence of nanoparticles on heat transfer, as was carried out in [57].

**Funding:** This research received no external funding.

**Conflicts of Interest:** The authors declare no conflict of interest.

## Nomenclature

|                                 |                                   |                        |
|---------------------------------|-----------------------------------|------------------------|
| $a$                             | Thermal diffusivity               | (m <sup>2</sup> /s)    |
| $d_f$                           | Base fluid molecule diameter      | (m)                    |
| $d_p$                           | Particle diameter                 | (m)                    |
| $D$                             | Inside diameter of tube           | (m)                    |
| $\bar{h}$                       | Average heat transfer coefficient | (W/(m <sup>2</sup> K)) |
| $k$                             | Thermal conductivity              | (W/(m K))              |
| $Nu = \frac{hD}{k}$             | Local Nusselt number              | (-)                    |
| $\bar{Nu} = \frac{\bar{h}D}{k}$ | Average Nusselt number            | (-)                    |
| $Pe = RePr$                     | Peclet number                     | (-)                    |
| $Pr = \frac{\nu}{a}$            | Prandtl number                    | (-)                    |
| $q$                             | Heat flux                         | (W/m <sup>2</sup> )    |
| $Rr = \frac{uD}{\nu}$           | Reynolds number                   | (-)                    |
| $u$                             | Velocity                          | (m/s)                  |
| $x$                             | Axial coordinate                  | (m)                    |

## Greek symbols

|           |                            |                     |
|-----------|----------------------------|---------------------|
| $\nu$     | Kinematic viscosity        | (m <sup>2</sup> /s) |
| $\varphi$ | Nanoparticle concentration | (-)                 |

## Subscripts

|    |           |
|----|-----------|
| In | Inlet     |
| m  | Mass      |
| nf | Nanofluid |
| p  | Particle  |
| v  | Volume    |
| w  | Wall      |

## Abbreviations

|             |   |
|-------------|---|
| 1Phase con. | Single phase model with constant properties       |
| 1PhaseD1    | Single phase model with thermal dispersion effect |
| 1PhaseD2    | Single phase model with thermal dispersion effect |
| 1Phase var. | Single phase model with variable properties       |
| AHTCD       | Average heat transfer coefficient enhancement     |
| AHTCE       | Average heat transfer coefficient enhancement     |
| ANuNE       | Average nu number enhancement                     |

|           |   |
|-----------|---|
| ASSI      | Average shear stress increase                         |
| ATF       | Automatic transmission fluid                          |
| AWSSI     | Average wall shear stress increase                    |
| BCon      | Boundary conditions                                   |
| CFD       | Computational fluid dynamics                          |
| CNT       | Carbon nanotubes                                      |
| CPU       | Computational processing unit                         |
| DPM       | Discrete phase model                                  |
| DPM con.  | Discrete phase model with constant properties         |
| DPM var.  | Discrete phase model with variable properties         |
| E         | Eulerian  |
| E-E       | Eulerian–Eulerian model                               |
| E-Mixture | Eulerian–mixture model                                |
| EG        | Ethylene glycol                                       |
| ExHTC     | Experimental heat transfer coefficient                |
| FC        | Friction coefficient                                  |
| FCI       | Friction coefficient increase                         |
| FF        | Friction factor                                       |
| FFI       | Friction factor increase                              |
| FDHTCE    | Fully developed heat transfer coefficient enhancement |
| FDWSSI    | Fully developed wall shear stress increase            |
| G         | Graphite  |
| GO        | Graphene oxide  |
| HFI       | Heat flux increase                                    |
| HTC       | Heat transfer coefficient                             |
| HTCE      | Heat transfer coefficient enhancement                 |
| HTCD      | Heat transfer coefficient deterioration               |
| HTNI      | Heat transfer negligible impact                       |
| FF        | Friction factor                                       |
| FFI       | Friction factor increase                              |
| NHTC      | Numerical heat transfer coefficient                   |
| NPC       | Nanoparticle concentration                            |
| NuND      | Nusselt number deterioration                          |
| NuNE      | Nusselt number enhancement                            |
| PD        | Pressure drop   |
| PDD       | Pressure drop decrease                                |
| PDI       | Pressure drop increase                                |
| PP        | Pumping power   |
| PPD       | Pumping power decrease                                |
| PPI       | Pumping power increase                                |
| RNG       | Re-normalization group                                |
| RSM       | Reynolds stress model                                 |
| TD        | Temperature decrease                                  |
| TNT       | Titanate  |
| VOF       | Volume of fluid                                       |
| WSS       | Wall shear stress                                     |
| WSSI      | Wall shear stress increase                            |

## References

1. Webb, R.L. *Principles of Enhanced Heat Transfer*; John Wiley&Sons, Inc.: New York, NY, USA, 1994.
2. Mousa, M.H.; Miljkovic, N.; Nawaz, K. Review of heat transfer enhancement techniques for single phase flows. *Renew. Sust. Energ. Rev.* **2021**, *137*, 110566. [[CrossRef](#)]
3. Gupta, M.; Singh, V.; Kumar, R.; Said, Z. A review on thermophysical properties of nanofluids and heat transfer applications. *Renew. Sust. Energ. Rev.* **2017**, *74*, 638–670. [[CrossRef](#)]



4. Angayarkanni, S.A.; Philip, J. Review on thermal properties of nanofluids: Recent developments. *Adv. Colloid Interface Sci.* **2015**, *225*, 146–176. [[CrossRef](#)] [[PubMed](#)]
5. Ilyas, S.U.; Pendyala, R.; Marneni, N. Stability of nanofluids. Topics in Mining, Metallurgy and Materials Engineering. In *Engineering Applications of Nanotechnology. From Energy to Drug Delivery*; Korada, V.S., Hamid, N.H.B., Eds.; Springer: Berlin/Heidelberg, Germany, 2017. Available online: <https://www.springerprofessional.de/engineering-applications-of-nanotechnology/11992454> (accessed on 1 July 2022).
6. Abdullah, M.; Malik, S.R.; Iqbal, M.H.; Sajid, M.M.; Shad, N.A.; Hussain, S.Z.; Razzaq, W.; Javed, Y. Sedimentation and stabilization of nano-fluids with dispersant. *Colloids Surf. A Physicochem. Eng. Asp.* **2018**, *554*, 86–92. [[CrossRef](#)]
7. Kamyar, A.; Saidur, R.; Hasanuzzaman, M. Application of Computational Fluid Dynamics (CFD) for nanofluids. *Int. J. Heat Mass Transf.* **2012**, *55*, 4104–4115. [[CrossRef](#)]
8. Kumar, S.; Chakrabarti, S. A Review: Enhancement of Heat Transfer with Nanofluids. *Int. J. Eng. Res. Technol.* **2014**, *3*, 549–557.
9. Kakaç, S.; Pramuanjaroenkij, A. Single-phase and two-phase treatments of convective heat transfer enhancement with nanofluids—A state-of-the-art review. *Int. J. Therm. Sci.* **2016**, *100*, 75–97. [[CrossRef](#)]
10. Mahian, O.; Kolsi, L.; Amani, M.; Estellé, P.; Ahmadi, G.; Kleinstreuer, C.; Marshall, J.S.; Siavashi, M.; Taylor, R.A.; Niazmad, H.; et al. Recent advances in modeling and simulation of nanofluid flows-Part I: Fundamentals and theory. *Phys. Rep.* **2019**, *790*, 1–48. [[CrossRef](#)]
11. Mahian, O.; Kolsi, L.; Amani, M.; Estellé, P.; Ahmadi, G.; Kleinstreuer, C.; Marshall, J.S.; Taylor, R.A.; Abu-Nada, E.; Rashidi, S.; et al. Recent advances in modeling and simulation of nanofluid flows-Part II: Applications. *Phys. Rep.* **2019**, *791*, 1–59. [[CrossRef](#)]
12. Maïga, S.; Nguyen, C.T.; Galanis, N.; Roy, G. Heat transfer behaviours of nanofluids in a uniformly heated tube. *Superlattices Microstruct.* **2004**, *35*, 543–557. [[CrossRef](#)]
13. Maïga, S.; Palm, S.J.; Nguyen, C.T.; Roy, G.; Galanis, N. Heat transfer enhancement by using nanofluids in forced convection flows. *Int. J. Heat Fluid Flow.* **2005**, *26*, 530–546. [[CrossRef](#)]
14. Maïga, S.; Nguyen, C.T.; Galanis, N.; Roy, G.; Maré, T.; Coqueux, M. Heat transfer enhancement in turbulent tube flow using Al<sub>2</sub>O<sub>3</sub> nanoparticle suspension. *Int. J. Numer. Methods Heat Fluid Flow* **2006**, *16*, 275–292. [[CrossRef](#)]
15. Heris, S.Z.; Esfahany, M.N.; Etemad, G. Numerical Investigation of Nanofluid Laminar Convective Heat Transfer through a Circular Tube. *Numer. Heat Transf. A Appl.* **2007**, *52*, 1043–1058. [[CrossRef](#)]
16. Behzadmehr, A.; Saffar-Avval, M.; Galanis, N. Prediction of turbulent forced convection of a nanofluid in a tube with uniform heat flux using a two phase approach. *Int. J. Heat Fluid Flow* **2007**, *28*, 211–219. [[CrossRef](#)]
17. Bianco, V.; Manca, O.; Nardini, S. Numerical investigation of transient single phase forced convection of nanofluids in circular tubes. *WIT Trans. Eng. Sci.* **2008**, *61*, 3–12.
18. Bianco, V.; Chiacchio, F.; Manca, O.; Nardini, S. Numerical investigation of nanofluids forced convection in circular tubes. *Appl. Therm. Eng.* **2009**, *29*, 3632–3642. [[CrossRef](#)]
19. He, Y.; Men, Y.; Zhao, Y.; Lu, H.; Ding, Y. Numerical investigation into the convective heat transfer of TiO<sub>2</sub> nanofluids flowing through a straight tube under the laminar flow conditions. *Appl. Therm. Eng.* **2009**, *29*, 1965–1972. [[CrossRef](#)]
20. Namburu, P.K.; Das, D.K.; Tanguturi, K.M.; Vajjha, R.S. Numerical study of turbulent flow and heat transfer characteristics of nanofluids considering variable properties. *Int. J. Therm. Sci.* **2009**, *48*, 290–302. [[CrossRef](#)]
21. Fard, M.H.; Esfahany, M.N.; Talaie, M.R. Numerical study of convective heat transfer of nanofluids in a circular tube two-phase model versus single-phase model. *Int. Commun. Heat Mass Transf.* **2010**, *37*, 91–97. [[CrossRef](#)]
22. Lotfi, R.; Saboohi, Y.; Rashidi, A.M. Numerical study of forced convective heat transfer of Nanofluids: Comparison of different approaches. *Int. Commun. Heat Mass Transf.* **2010**, *37*, 74–78. [[CrossRef](#)]
23. Mokmeli, A.; Saffar-Avval, M. Prediction of nanofluid convective heat transfer using the dispersion model. *Int. J. Therm. Sci.* **2010**, *49*, 471–478. [[CrossRef](#)]
24. Ebrahimi-Bajestan, E.; Niazmand, H.; Duangthongsuk, W.; Wongwises, S. Numerical investigation of effective parameters in convective heat transfer of nanofluids flowing under a laminar flow regime. *Int. J. Heat Mass Transf.* **2011**, *54*, 4376–4388. [[CrossRef](#)]
25. Moraveji, M.K.; Darabi, M.; Haddad, S.M.H.; Davarnejad, R. Modeling of convective heat transfer of a nanofluid in the developing region of tube flow with computational fluid dynamics. *Int. Commun. Heat Mass Transf.* **2011**, *38*, 1291–1295. [[CrossRef](#)]
26. Bianco, V.; Manca, O.; Nardini, S. Numerical investigation on nanofluids turbulent convection heat transfer inside a circular tube. *Int. J. Therm. Sci.* **2011**, *50*, 341–349. [[CrossRef](#)]
27. Bayat, J.; Nikseresht, A.H. Investigation of the different base fluid effects on the nanofluids heat transfer and pressure drop. *Heat Mass Transf.* **2011**, *47*, 1089–1099. [[CrossRef](#)]
28. Akbari, M.; Galanis, N.; Behzadmehr, A. Comparative analysis of single and two-phase models for CFD studies of nanofluid heat transfer. *Int. J. Therm. Sci.* **2011**, *50*, 1343–1354. [[CrossRef](#)]
29. Akbari, M.; Galanis, N.; Behzadmehr, A. Comparative assessment of single and two-phase models for numerical studies of nanofluid turbulent forced convection. *Int. J. Heat Fluid Flow.* **2012**, *37*, 136–146. [[CrossRef](#)]
30. Alvarino, P.F.; Jabardo, J.M.S.; Arce, A.; Galdo, M.I.L. Heat transfer enhancement in nanofluids. A numerical approach. *J. Phys. Conf. Ser.* **2012**, *395*, 012116. [[CrossRef](#)]

31. Tahir, S.; Mital, M. Numerical investigation of laminar nanofluid developing flow and heat transfer in a circular channel. *Appl. Therm. Eng.* **2012**, *39*, 8–14. [[CrossRef](#)]
32. Balla, H.H.; Abdullah, S.; Zulkifli, R. Effect of oxides nanoparticles materials on the pressure loss and heat transfer on nanofluids in circular pipes. *J. Appl. Sci.* **2012**, *12*, 1396–1401. [[CrossRef](#)]
33. Bayat, J.; Nikseresht, A.H. Thermal performance and pressure drop analysis of nanofluids in turbulent forced convective flows. *Int. J. Therm. Sci.* **2012**, *60*, 236–243. [[CrossRef](#)]
34. Moraveji, M.K.; Esmaeili, E. Comparison between Single-Phase and Two-Phases CFD Modeling of Laminar Forced Convection Flow of Nanofluids in Circular Tube under Constant Heat Flux. *Int. Commun. Heat Mass Transf.* **2012**, *39*, 1297–1302. [[CrossRef](#)]
35. Davarnejad, R.; Barati, S.; Zakeri, M. Simulation of Convective Heat Transfer of a Nanofluid in a Circular Cross-section. *Int. J. Eng.* **2013**, *26*, 571–576. [[CrossRef](#)]
36. Davarnejad, R.; Barati, S.; Kooshki, M. CFD simulation of the effect of particle size on the nanofluids convective heat transfer in the developed region in a circular tube. *Springerplus* **2013**, *2*, 192. [[CrossRef](#)] [[PubMed](#)]
37. Kayaci, N.; Balcilar, M.; Tabatabaei, M.; Celen, A.; Yıldız, O.; Dalkilic, A.S.; Wongwises, S. Determination of the Single-Phase Forced Convection Heat Transfer Characteristics of TiO<sub>2</sub> Nanofluids Flowing in Smooth and Micro-Fin Tubes by Means of CFD and ANN Analyses. *Curr. Nanosci.* **2013**, *9*, 61–80.
38. Hejazian, M.; Moraveji, M.K. A Comparative Analysis of Single and Two-Phase Models of Turbulent Convective Heat Transfer in a Tube for TiO<sub>2</sub> Nanofluid with CFD. *Numer. Heat Transf. A Appl.* **2013**, *63*, 795–806. [[CrossRef](#)]
39. Göktepe, S.; Atalık, K.; Ertürk, H. Comparison of single and two-phase models for nanofluid convection at the entrance of a uniformly heated tube. *Int. J. Therm. Sci.* **2014**, *80*, 83–92. [[CrossRef](#)]
40. Saha, G.; Paul, M.C. Numerical analysis of the heat transfer behaviour of water based Al<sub>2</sub>O<sub>3</sub> and TiO<sub>2</sub> nanofluids in a circular pipe under the turbulent flow condition. *Int. Commun. Heat Mass Transf.* **2014**, *56*, 96–108. [[CrossRef](#)]
41. Bianco, V.; Manca, O.; Nardini, S. Performance analysis of turbulent convection heat transfer of Al<sub>2</sub>O<sub>3</sub> water-nanofluid in circular tubes at constant wall temperature. *Energy* **2014**, *77*, 403–413. [[CrossRef](#)]
42. Saha, G.; Paul, M.C. Heat transfer and entropy generation of turbulent forced convection flow of nanofluids in a heated pipe. *Int. Commun. Heat Mass Transf.* **2015**, *61*, 26–36. [[CrossRef](#)]
43. Aghaei, A.; Sheikhzadeh, G.A.; Dastmalchi, M.; Forozande, H. Numerical investigation of turbulent forced-convective heat transfer of Al<sub>2</sub>O<sub>3</sub>–water nanofluid with variable properties in tube. *Ain Shams Eng. J.* **2015**, *6*, 577–585. [[CrossRef](#)]
44. Minea, A.A. Simulation of Nanofluids Turbulent Forced Convection at High Reynolds Number: A Comparison Study of Thermophysical Properties Influence on Heat Transfer Enhancement. *Flow Turbul Combust.* **2015**, *94*, 555–575. [[CrossRef](#)]
45. Nasiri-lohesara, M. Heat Transfer Enhancement and Hydrodynamic Characteristics of Nanofluid in Turbulent Flow Regime. *J. Energy* **2015**, *2015*, 814717. [[CrossRef](#)]
46. Ehsan, M.M.; Noor, S. Study of Heat Transfer Performance and Pumping Power Improvement of Nanofluid Through a Rough Circular Tube. *Int. Res. J. Eng. Technol.* **2016**, *3*, 1709–1717.
47. Mahdavi, M.; Sharifpur, M.; Meyer, J.P. Simulation study of convective and hydrodynamic turbulent nanofluids by turbulence models. *Int. J. Therm. Sci.* **2016**, *110*, 36–51. [[CrossRef](#)]
48. Purohit, N.; Purohit, V.A.; Purohit, K. Assessment of nanofluids for laminar convective heat transfer: A numerical study. *Eng. Sci. Technol. Int. J.* **2016**, *19*, 574–586. [[CrossRef](#)]
49. Jahanbin, A. Comparative Study on Convection and Wall Characteristics of Al<sub>2</sub>O<sub>3</sub>–Water Nanofluid Flow inside a Miniature Tube. *Eng. J.* **2017**, *20*, 169–181. [[CrossRef](#)]
50. Elahmer, M.; Abboudi, S.; Boukadida, N. Nanofluid effect on forced convective heat transfer inside a heated horizontal tube. *Int. J. Heat Technol.* **2017**, *35*, 874–882. [[CrossRef](#)]
51. Albojamal, A.; Vafai, K. Analysis of single phase, discrete and mixture models, in predicting nanofluid transport. *Int. J. Heat Mass Transf.* **2017**, *108*, 225–237. [[CrossRef](#)]
52. Rashidi, M.M.; Nasiri, M.; Shadloo, M.S.; Yang, Z. Entropy Generation in a Circular Tube Heat Exchanger Using Nanofluids: Effects of Different Modeling Approaches. *Heat Transf. Eng.* **2017**, *38*, 853–866. [[CrossRef](#)]
53. Rabby, I.I.; Amin, S.A.M.S.; Rahman, S.; Islam, A.K.M.S. Numerical Investigation of Laminar Convective Heat Transfer and Friction Factor of a Pipe by Using Al<sub>2</sub>O<sub>3</sub>-Water Nanofluid. In Proceedings of the International Conference on Mechanical, Industrial and Energy Engineering, Khulna, Bangladesh, 23–24 December 2018.
54. Boertz, H.; Baars, A.J.; Cieśliński, J.T.; Smolen, S. Numerical Study of Turbulent Flow and Heat Transfer of Nanofluids in Pipes. *Heat Transf. Eng.* **2018**, *39*, 241–251. [[CrossRef](#)]
55. Kristiawan, B.; Santoso, B.; Wijayanta, A.T.; Aziz, M.; Miyazaki, T. Heat Transfer Enhancement of TiO<sub>2</sub>/Water Nanofluid at Laminar and Turbulent Flows: A Numerical Approach for Evaluating the Effect of Nanoparticle Loadings. *Energies* **2018**, *11*, 1584. [[CrossRef](#)]
56. Sajjad, M.; Kamran, M.S.; Shaukat, R.; Zeinelabdeen, M.I.M. Numerical investigation of laminar convective heat transfer of graphene oxide/ethylene glycol-water nanofluids in a horizontal tube. *Eng. Sci. Technol. Int. J.* **2018**, *21*, 727–735. [[CrossRef](#)]
57. Minea, A.A.; Buonomo, B.; Burggraf, J.; Ercole, D.; Karpaiya, K.R.; Di Pasqua, A.; Sekrani, G.; Steffens, J.; Tibaut, J.; Wichmann, N.; et al. NanoRound: A benchmark study on the numerical approach in nanofluids' simulation. *Int. Commun. Heat Mass Transf.* **2019**, *108*, 104292. [[CrossRef](#)]

58. Onyiriuka, E.J.; Ikponmwoba, E.A.A. Numerical investigation of mango leaves-water nanofluid under laminar flow regime. *Niger. J. Technol.* **2019**, *38*, 348–354. [[CrossRef](#)]
59. Jamali, M.; Toghraie, D. Investigation of heat transfer characteristics in the developing and the developed flow of nanofluid inside a tube with different entrances in the transition regime. *J. Therm. Anal. Calorim.* **2020**, *139*, 685–699. [[CrossRef](#)]
60. Fadodun, O.G.; Amosun, A.A.; Salau, A.O.; Olaloye, D.O.; Ogundeji, J.A.; Ibitoye, F.I.; Balogun, F.A. Numerical investigation and sensitivity analysis of turbulent heat transfer and pressure drop of  $\text{Al}_2\text{O}_3/\text{H}_2\text{O}$  nanofluid in straight pipe using response surface methodology. *Arch. Thermodyn.* **2020**, *41*, 3–30.
61. Saeed, F.R.; Al-Dulaimi, M.A. Numerical investigation for convective heat transfer of nanofluid laminar flow inside a circular pipe by applying various models. *Arch. Thermodyn.* **2021**, *42*, 71–95.
62. Uribe, S.; Zouli, N.; Cordero, M.E.; Al-Dahhan, M. Development and validation of a mathematical model to predict the thermal behaviour of nanofluids. *Heat Mass Transf.* **2021**, *57*, 93–110. [[CrossRef](#)]
63. Taskesen, E.; Tekir, M.; Gedik, E.; Arslan, K. Numerical investigation of laminar forced convection and entropy generation of  $\text{Fe}_3\text{O}_4$ /water nanofluids in different cross-sectioned channel geometries. *J. Therm. Eng.* **2021**, *7*, 1752–1767. [[CrossRef](#)]
64. Yildiz, M.; Aktürk, A. Numerical Investigation on Heat Transfer and Hydraulic Performance of  $\text{Al}_2\text{O}_3$ -Water Nanofluid as a Function of Reynolds Number and Flow Velocity. *Int. J. Heat Mass Transf.* **2021**, *11*, 535–547. [[CrossRef](#)]
65. Buongiorno, J. Convective Transport in Nanofluids. *Int. J. Heat Trans.* **2006**, *128*, 240–250. [[CrossRef](#)]
66. Williams, W.; Buongiorno, J.; Hu, L.W. Experimental Investigation of Turbulent Convective Heat Transfer and Pressure Loss of Alumina/Water and Zirconia/Water Nanoparticle Colloids (Nanofluids) in Horizontal Tubes. *J. Heat Trans.* **2008**, *130*, 042412. [[CrossRef](#)]
67. Sommers, A.D.; Yerkes, K.L. Experimental investigation into the convective heat transfer and system-level effects of  $\text{Al}_2\text{O}_3$ -propanol nanofluid. *J. Nanopart Res.* **2009**, *12*, 1003–1014. [[CrossRef](#)]
68. Sahin, B.; Manay, E.; Akyurek, E.F. An Experimental Study on Heat Transfer and Pressure Drop of CuO-Water Nanofluid. *J. Nanomater.* **2015**, *16*, 790839. [[CrossRef](#)]
69. Zhang, X.; Li, J. A review of uncertainties in the study of heat transfer properties of nanofluids. *Heat Mass Transf.* **2022**, 1–33. [[CrossRef](#)]
70. Buongiorno, J.; Venerus, D.C.; Prabhat, N.; McKrell, T.J.; Townsend, J.; Christianson, R.J.; Tolmachev, Y.V.; Keblinski, P.; Hu, L.-W.; Alvarado, J.L.; et al. A benchmark study on the thermal conductivity of nanofluids. *J. Appl. Phys.* **2009**, *106*, 094312. [[CrossRef](#)]

